

# Containing the Liquid in Liquid Lenses

Gerard Desroches

OPTI523L – Independent Project – Final Report

April 28, 2009

## 1. Introduction

Liquid lenses are gaining popularity in optical systems due to their dynamic nature. When designed properly they can athermalize optical systems, be used in zoom configurations without the need for additional mechanics or even provide chromatic correction. Because they are liquid, they can also conform to any volume they are placed in which also allows for potentially new geometries to be used in optical systems.

This report provides an analysis of temperature effects on a simple optical glass-liquid cell. Since optical liquids have abnormally large coefficients of thermal expansion compared to glass and metals, an expansion bladder was incorporated into the cell design to allow the optical liquid to expand freely without adding pressure within the glass cavity. This was done in order to determine whether residual optical power due to thermal effects needed to be compensated for in a more complex cell.

## 2. Some Background Information

An unusual property of optical liquids is an extremely large refractive index change with temperature, or  $dn/dT$ . In order to minimize local refractive index variations within the liquid, thin liquid lenses are normally used to minimize the volume thereby minimizing temperature gradients within the volume. Gradients show up as undesired local variations in the final image. For this experiment, the cell was thermally ‘soaked’ so that all the components and the optical liquid could be tested at a uniform temperature.

Optical liquids can be selected by refractive index and dispersion just as optical glass. They can also be selected by other properties such as useful transmission range, viscosity and density to name a few. In this case, the optical liquid was selected to closely match the refractive index of the windows that encompass the liquid. This was done to ensure that when measuring the cell in a double-pass interferometer test, magnification of errors due to refractive index effects would be eliminated. Curvature of the windows due to pressure and thermal effects would simply show up as ‘power’ in the interferometer test.

Since the windows to be used were made of B270 glass from Schott, the refractive index and dispersion of this material is quite close to BK7, also from Schott. A commercially available BK7 matching liquid from Cargille Laboratories was used that made the internal glass surfaces virtually transparent for the testing.

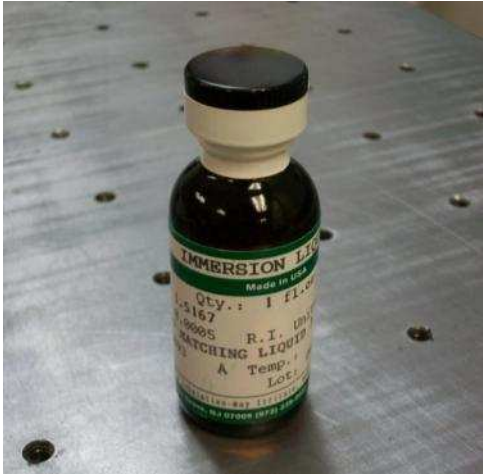


**Figure 1: BK7 matching liquid**

**3. The Optical Liquid Cell**

This simple version of a liquid cell was made from the following components:

Quantity	Component	Material
2	Window	B270
1	Cell Barrel	Anodized Aluminum
2	Retaining Rings	Brass

**Table 1: Liquid cell components**

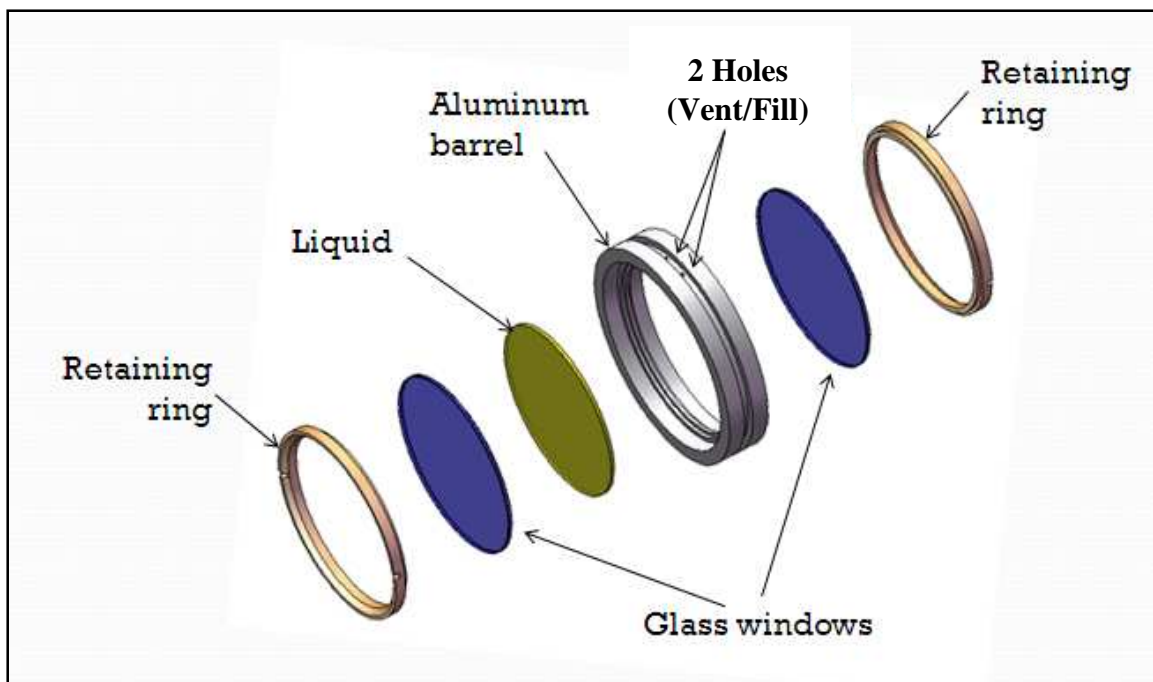


**Figure 2: Exploded view of the liquid cell assembly**

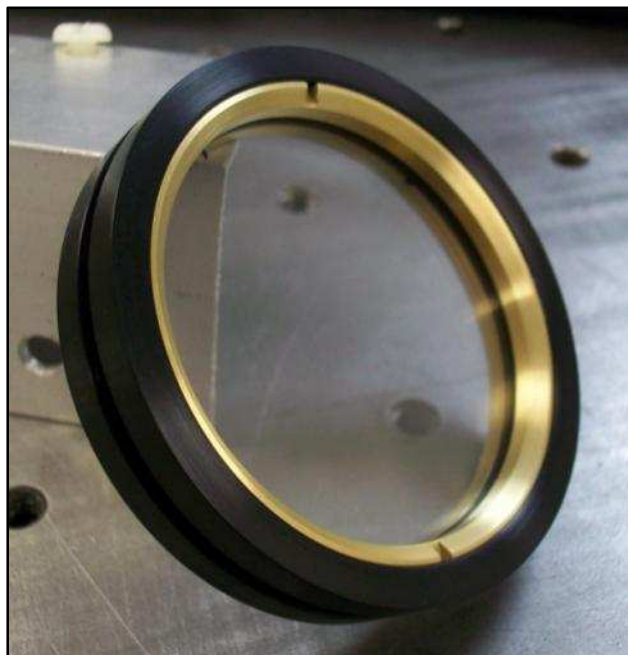


**Figure 3: Assembled cell**

The windows of the cell were bonded with RTV 157. This ensured that a good liquid-proof seal was in place. The expansion bladder was simply a stainless steel pipe bonded into one of the vent/fill holes in the barrel. A length of clear tubing was placed over the pipe and an open ended syringe was placed at the other end. With this makeshift expansion bladder, the optical liquid could expand freely without adding pressure within the cell's cavity. Obviously this open-ended expansion bladder is for testing purposes only. A more finalized design would make use of the groove in the outside edge of the cell barrel. This groove was intentionally put into the mechanical design as an area where an expansion bladder could be inserted to avoid interference with potential locating/mounting surfaces.

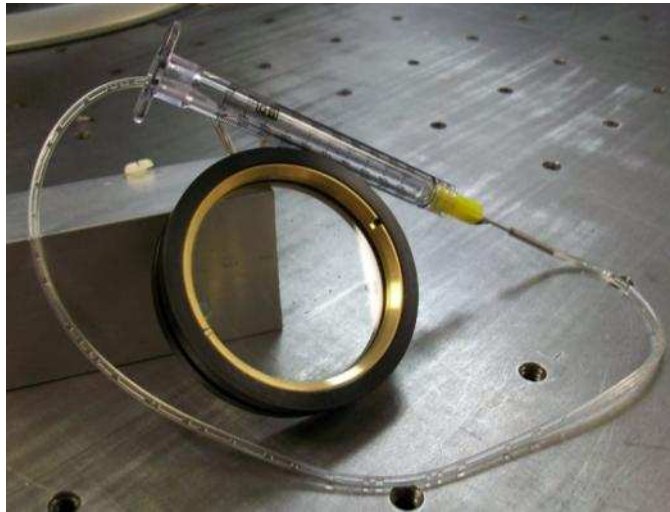


**Figure 4: Assembled cell and ‘expansion’ bladder**

Calculating the volume change of the optical liquid:

Liquid CTE =  $0.0007 \text{ cc/cc/}^\circ\text{C}$

Thickness of liquid layer = 1mm

Diameter of liquid cavity = 49mm

Temperature change =  $20^\circ\text{C}$

Total initial volume =  $1885.74 \text{ mm}^3$

Assuming the liquid will expand all directions the change in thickness and diameter becomes:

$$\Delta t = t\alpha\Delta T = 0.014mm$$

$$\Delta D = D\alpha\Delta T = 0.686mm$$

The new dimensions for the expanded volume are as follows:

Thickness of expanded liquid layer: 1.014mm

Expanded diameter of liquid: 49.686mm

Giving a new expanded volume of:  $1966.06mm^3$

This gives a total volume change of  $80.32mm^3$ .

To solve for one surface at a time, only half of this volume was used. This resulted in a surface bulge of 0.0426mm with the volume change.

This equates to a fringe difference of approximately 134 fringes @  $\lambda 632.8nm$  (HeNe)

Assuming the window can bend enough to comply with the entire volume change, the surface would have a radius of curvature of 7046.7mm. This bulge effect is also consistent with the FEA analysis done with COSMOS.

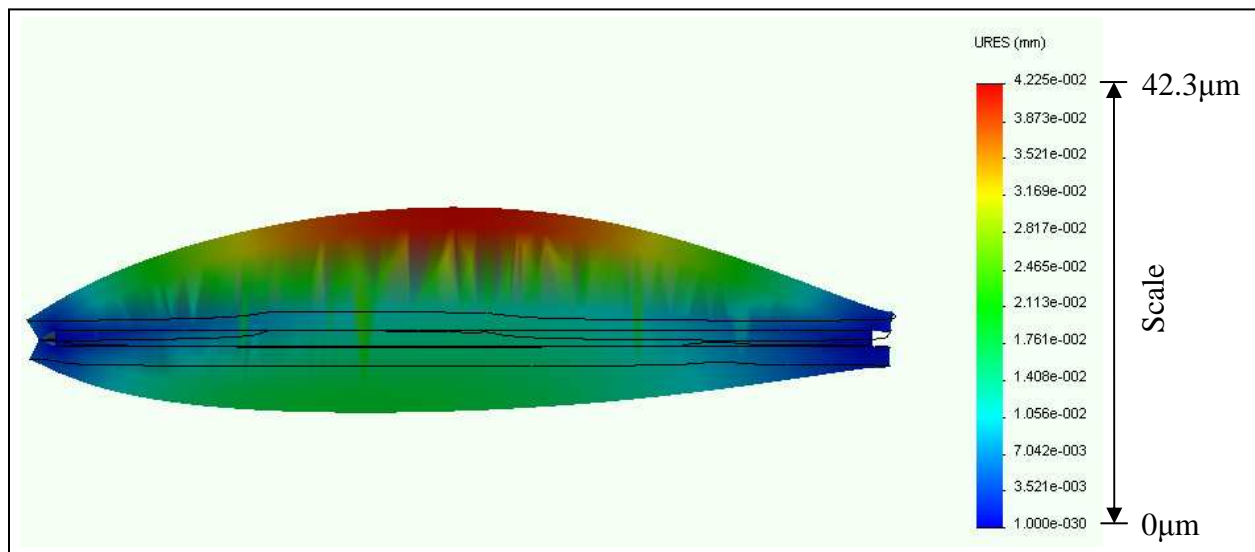


**Figure 5: FEA thermal analysis**

The change in power  $\phi$  can be calculated assuming a biconvex lens of refractive index  $n=1.517$  is formed due to the volume increase.

$$\phi = \phi_1 + \phi_2 - \phi_1\phi_2t = 0.0001467\text{mm}^{-1}$$

$$\text{focal length} = 1/\phi = 6815.2\text{mm} @ 40^\circ\text{C}$$

By symmetry, the focal length of the liquid lens would be approximately -6800mm (note change in sign) assuming the system will behave similarly when subjected to cold temperature. This change in power to a system caused by this element would introduce a shift in image position. This clearly shows an expansion bladder needs to be used.

#### 4. Thermal testing

In order to do interferometric testing, an environmental chamber had to be constructed. Details of the chamber can be found in the appendix.

Unfortunately the windows in the cell used were not very flat. Interferograms of the outer surfaces of the cell show how distorted the surfaces actually were prior to any testing. With such irregular surfaces, problems were anticipated in the testing of the complete cell. The rapid slope changes and strange artefacts showing up in the surface lead to misinterpretation of the fringe information by the interferometer software. Sharp 'steps' appear in the interferogram due to steep slopes in the surface and cause the surface map to look very odd.

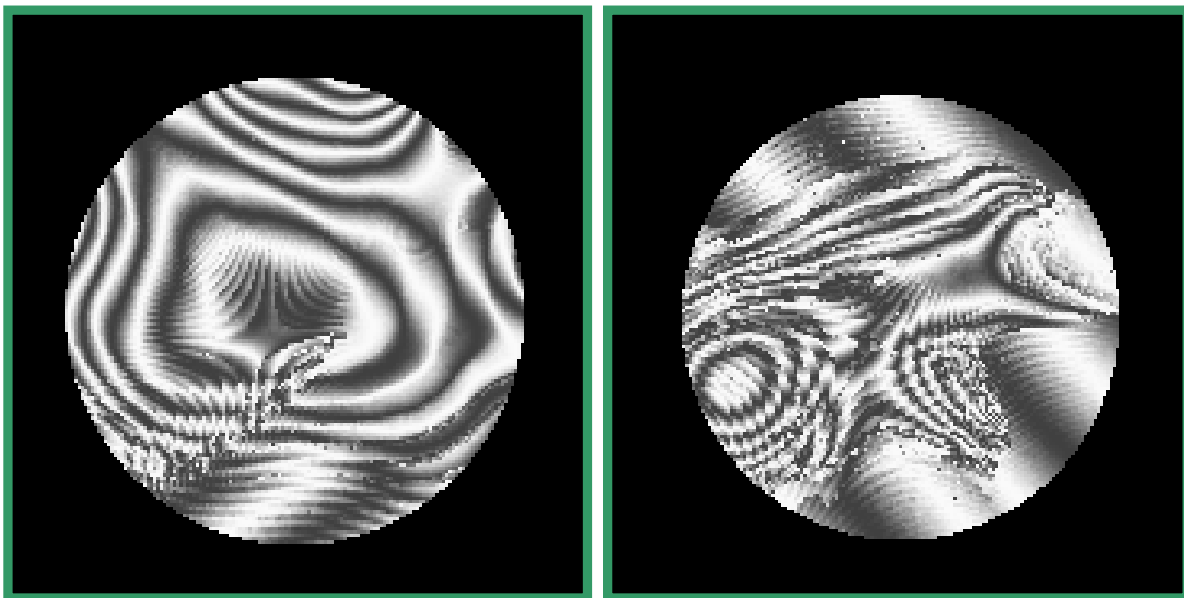


**Figure 6: Synthetic fringe maps of outer surfaces of cell**

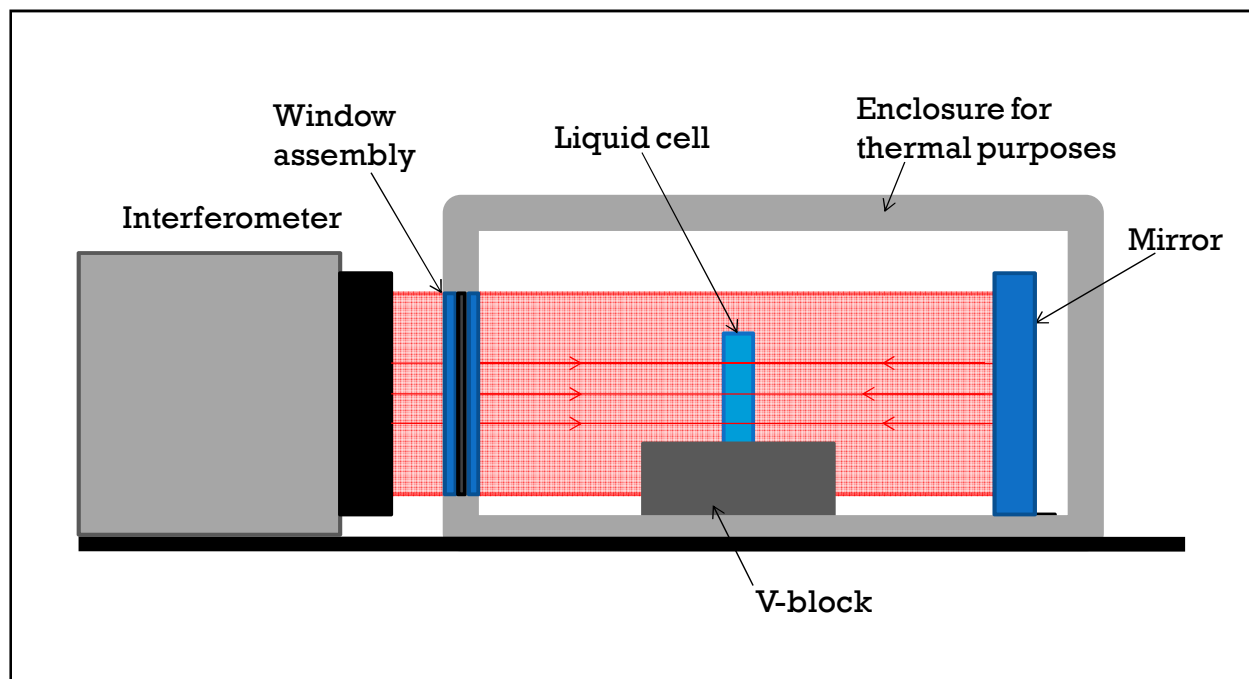


**Figure 7: Typical double pass interferometer test**

A similar test as the one shown in Figure 7 was used to measure the transmitted wavefront through the liquid cell. The actual test made use of a large 45° mirror to bend the ray path down. The liquid cell could simply be placed directly onto the flat mirror in the thermal chamber and the V-block would not be needed. In order to avoid front and rear face reflections that would interfere with the desired return image, the cell was tilted slightly to avoid being directly perpendicular to the incoming collimated beam. The actual test set-up is shown in Figure 8.

In order to determine the amount of residual power left in the thermally soaked cell, a measurement was taken at room temperature, approximately 23°C, and then again at the elevated temperature of 40°C. Unfortunately, time constraints did not allow for testing at cold temperatures.

The data was recorded using the interferometer software, but saved in a format that could be read into MetroPro for analysis.

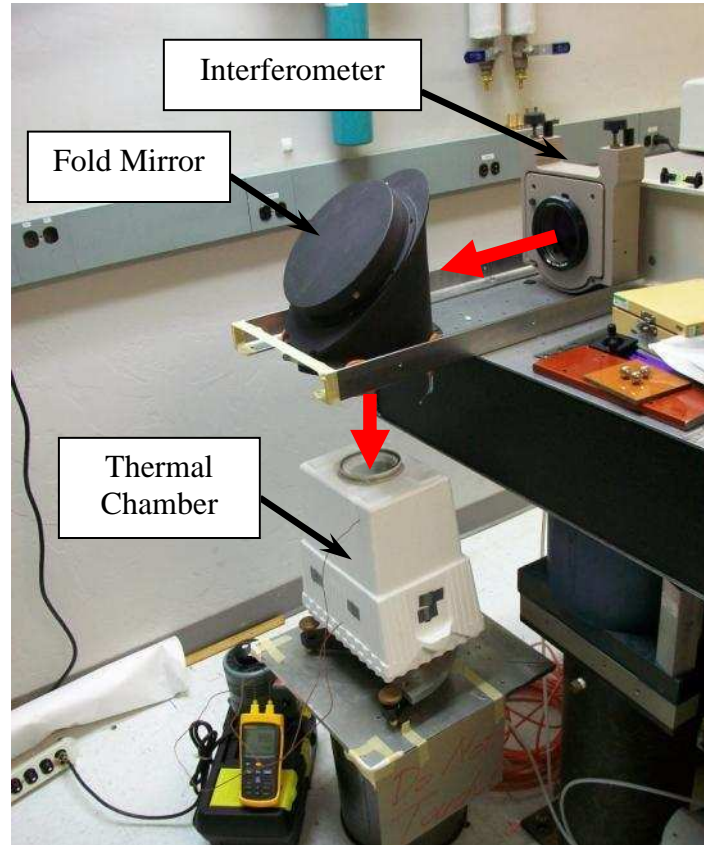


**Figure 8: Actual test set-up**

## **5. Interferometer results**

The images in Figure 9 and Figure 10 show synthetic fringe maps of actual interferograms taken of the transmitted wavefront error through the liquid cell. The mirror used in the thermal chamber was a testplate with a surface error less than  $\lambda/10$ . This small surface error was ignored in the measurement as it was included in both the ambient and elevated temperature measurements. In the subtracted result, the contribution of the testplate was in essence removed from the measurement, ignoring of course any thermal effect changes from that surface. Zernike terms are supplied in the appendix. (Figure 11: Zernike terms and Seidels for ambient measurement #1 Figure 11 – Figure 16)

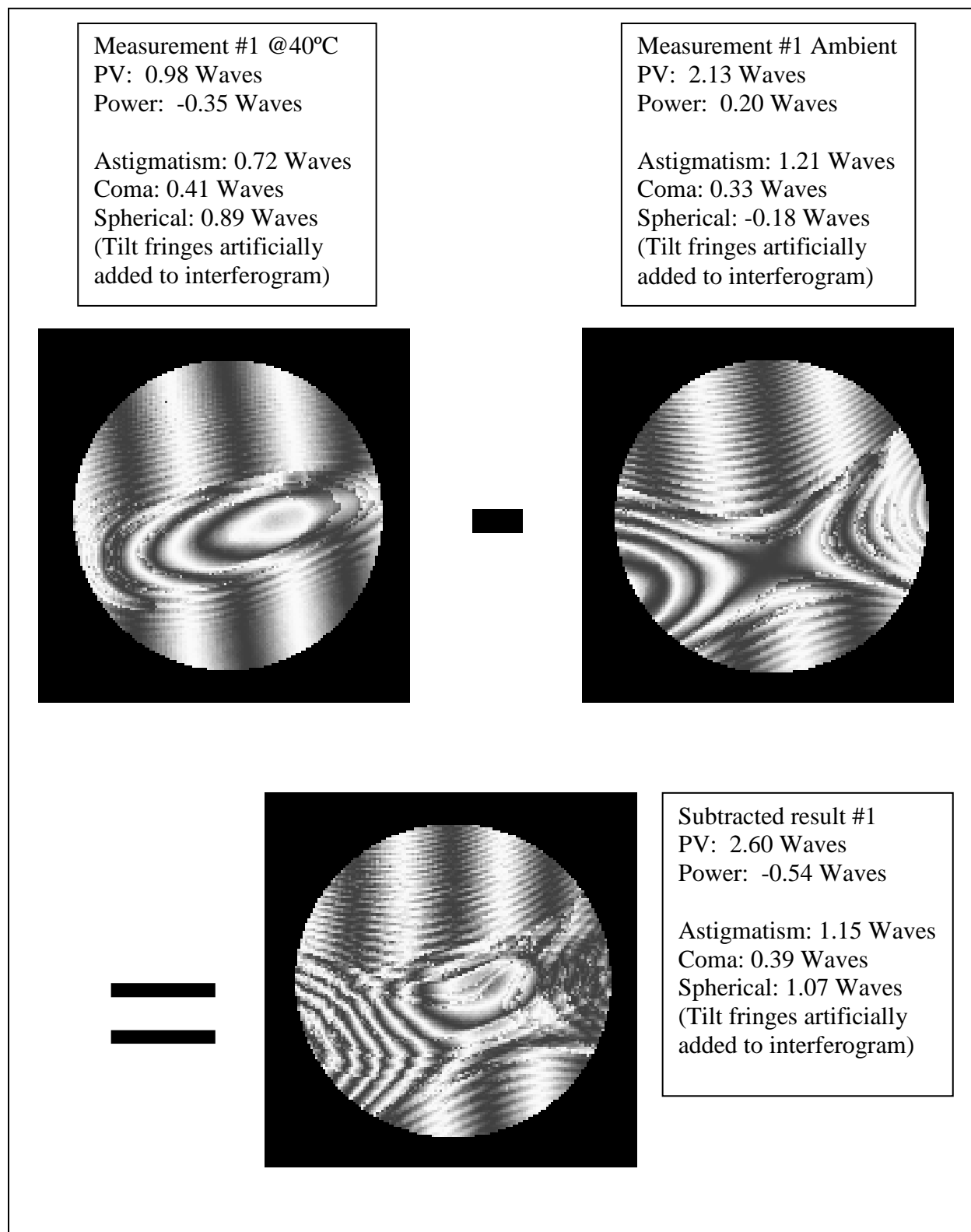


**Figure 9: Synthetic fringe map results from thermal test #1**

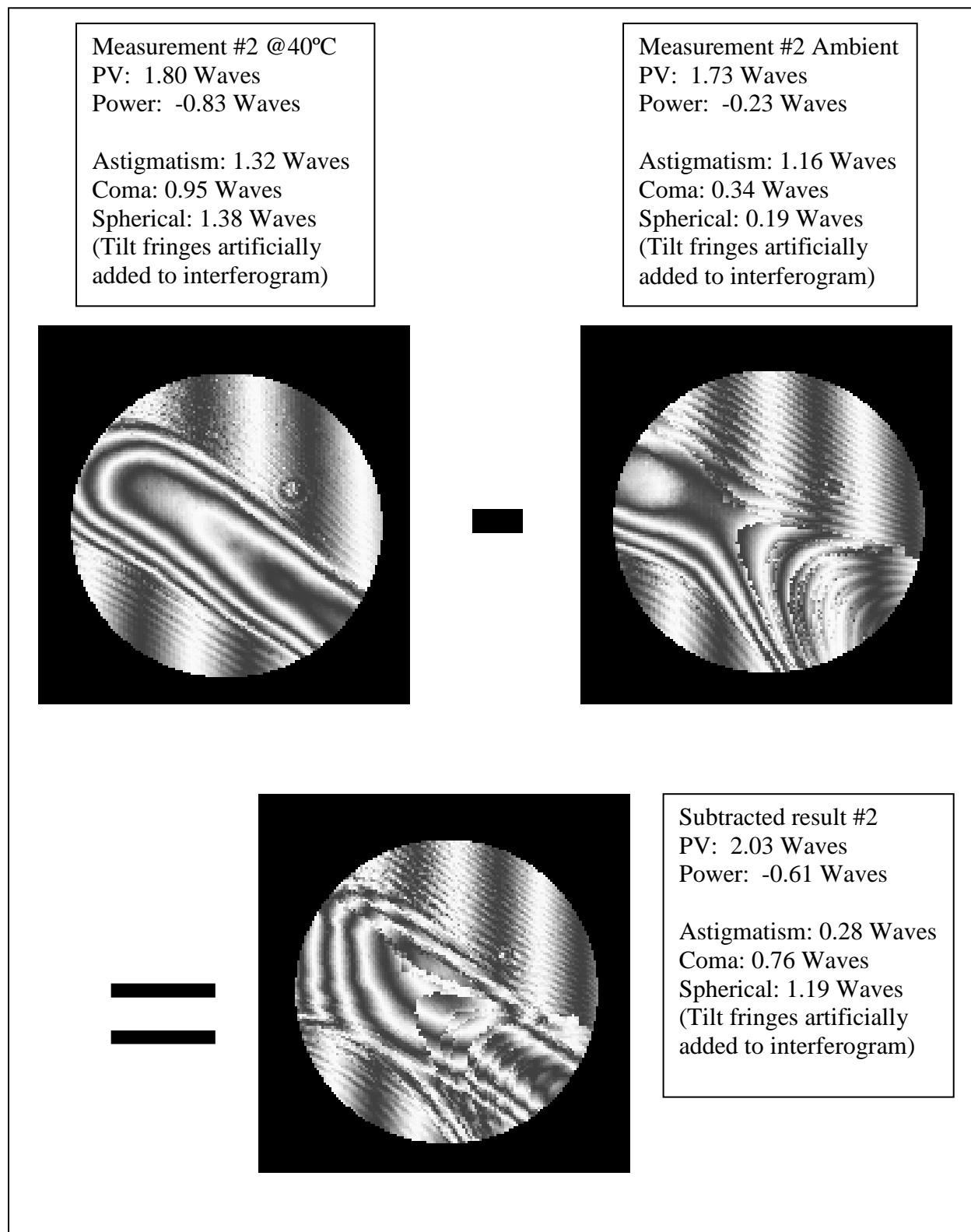


**Figure 10: Synthetic fringe map results from thermal test #2**

From Figure 9 and Figure 10, it is very apparent that the irregular surfaces of the windows are contributing to the transmitted wavefront error. But luckily, determining factor is the amount of power introduced by the temperature change. In both cases, the power in the subtracted interferogram shows slightly more than half a wave, -0.54 and -0.61 waves. The irregularity in both cases is still quite similar also. This implies that the expansion bladder was doing what it was intended to do; allow the optical liquid to expand freely without adding pressure within the cavity. If a pressure increase would have occurred, the result would have been additional power being measured in the transmitted wavefront interferometric test. Without the expansion bladder, the change in surface curvature would have been very noticeable, as calculated in section 3.

## **6. Improvements**

Using windows with less irregularity would be one of the most obvious improvements if this test was to be repeated. Data acquisition would be better without the steep slope errors noticed in these windows.

The use of a bell jar vacuum would have helped to get bubbles out of the thick index matching liquid, both from the bottle and in the cell. The time waiting for small bubbles to come up through the liquid and out the vent hole would have decreased if a vacuum was used. Initially evaporation was thought to be occurring but after blocking the holes it was clear that it was just slow moving, tiny bubbles taking longer to reach the top.

## 8. Conclusions

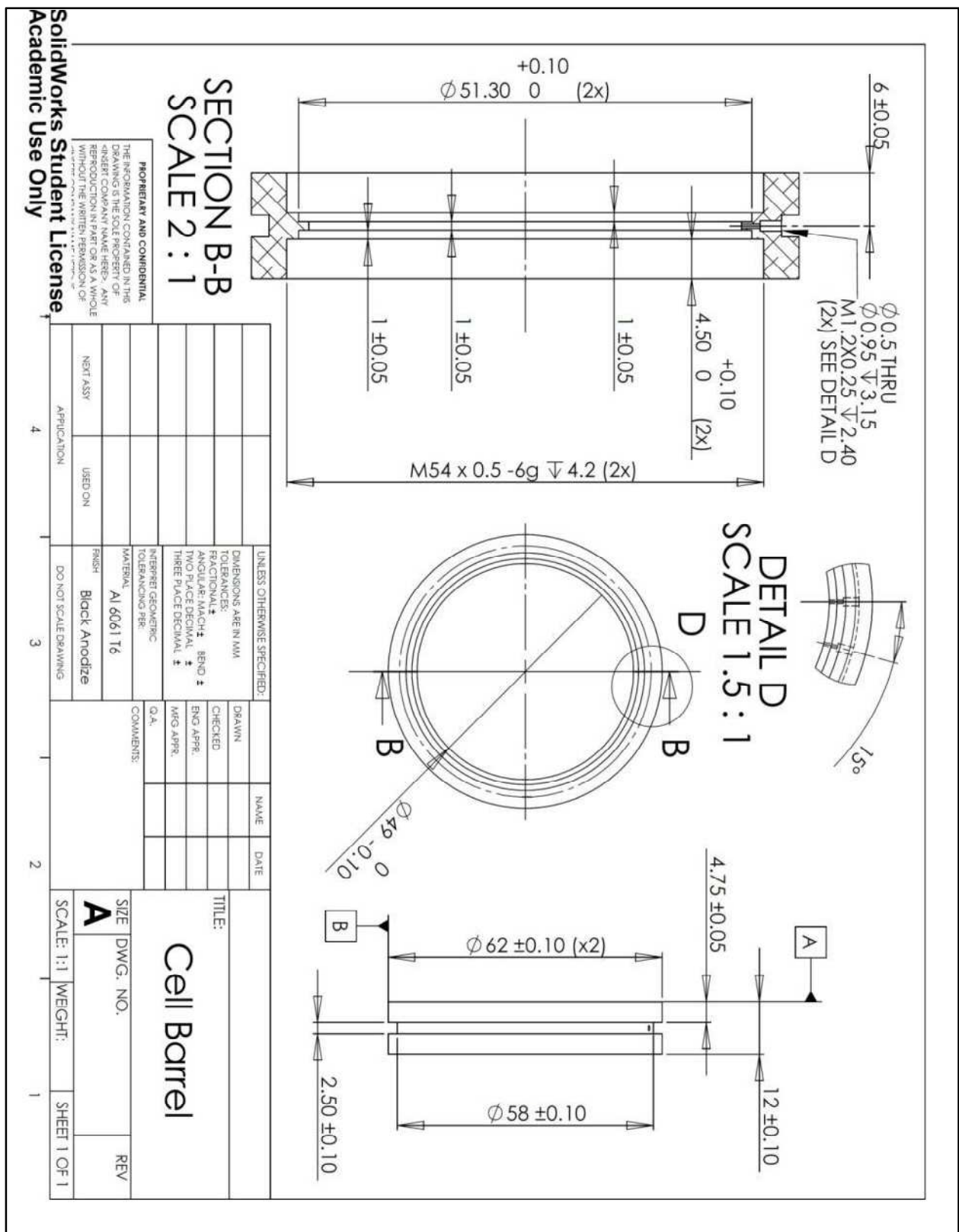
The goal of the experiment was to determine how much power would be introduced in a glass-liquid cell due to thermal effects when an expansion bladder is used. The live video interferogram did not change drastically as the thermal chamber heated up, implying that the expansion bladder was operating correctly by allowing the optical liquid to expand freely outside the glass cavity. The interferometric measurements showed slightly more than half a wave ( $\lambda/2$ ) of power was introduced (actual -0.54 and -0.61 waves) for a temperature increase of approximately 20°C.

Due to time constraints, cold temperature measurements were not performed. But assuming symmetry holds for the temperature limits, a power change of approximately half a wave ( $\lambda/2$ ) should also be observed going from ambient to 0°C. This implies that for the entire temperature range of 0°C to 40°C, the total change in power would be approximately one wave, which is a tolerable amount.

On another positive note, no leakage was observed in the liquid cell. Therefore, the sealing method used was adequate for this temperature range. Using RTV 156 with a bond gap of 0.3mm and held down with brass retaining rings provided the desired effect. Long term effects of the seals were not considered and not possible within the time allowed.

## 9. Appendix

<b>CARGILLE</b> <b>BK-7 MATCHING LIQUID CODE 11510</b> $n(5893 \text{ \AA}) 25 \text{ }^\circ\text{C} = 1.5167$ TYPICAL CHARACTERISTICS						
<u>COMPOSITION</u> .....	Phthalate Esters and Chlorinated Aliphatic Hydrocarbons					
<u>APPEARANCE</u> .....	Colorless to Slightly Yellow Liquid					
<u>INDEX CHANGE RATE BY EVAPORATION</u> .....	Very Low : 0.00000 expected, exposed					
surface area to volume ratio of 0.2 cm <sup>2</sup> / cc @ 25 °C for 37 days.						
<u>ODOR</u> .....	Very Slight					
<u>COLOR STABILITY</u> .....	In Sun: may slightly darken after 1 year; very slightly more after 6 years					
<u>POUR POINT</u> °C.....	- 10					
<u>BOILING POINT</u> °C @ 760mm Hg.....	Decomposes					
<u>FLASH POINT</u> °C COC.....	Decomposes at 160 °C					
<u>DENSITY</u> g / cc @ 25 °C.....	1.334					
<u>DENSITY TEMP. COEFFICIENT</u> g / cc / °C.....	-0.0010					
<u>COEF. OF THERM. EXP.</u> cc / cc / °C.....	0.0007					
<u>VISCOSITY</u> centistokes @ 25 °C.....	1,250 , ( ca. 2,910 @ 15 °C, 650 @ 35 °C )					
<u>SOLUBLE</u> : Acetone, Carbon Tetrachloride, Ethanol, Ethyl Ether, Heptane, Methylene Chloride, Naphtha, Toluene, Turpentine, Xylene						
<u>INSOLUBLE</u> : Water						
<u>COMPATIBLE</u> 10 month immersion @ 25 °C : Acrylic, Cellulose Acetate, Epoxy, Mylar, Nylon, Polyester, Polyethylene, Polypropylene, Polyurethane, Polyvinyl Chloride, Phenolic, Teflon, Silicone and Fluorosilicone Rubber, Latex Rubber; Aluminum, Copper, Brass, Steel; ( tests done on one example of each ).						
<u>INCOMPATIBLE</u> : Polycarbonate, Polystyrene, Neoprene Rubber and Tygon						
<u>TOXICITY</u> .....	Low ( request MSDS )					
<u>CAUCHY EQUATION</u> : refractive index as a function of wavelength at 25 °C						
W = wavelength in angstroms ( Å )						
$n(W) = 1.502787 + (455872.4) / W^2 + (9.844856E+11) / W^4$						
SOURCE OR SPECTRAL LINE	WAVELENGTH ( angstroms )	REFRACTIVE INDEX @ 25 °C		% TRANSMITTANCE		
		Liquid	BK-7	0.1 mm	1 mm	1 cm
near UV cut off	3100	1.561	1.549	97	75	6
i ( Hg )	3650	1.543	1.536	100	96	70
h ( Hg )	4047	1.5343	1.5302	100	99	91
F' ( Cd )	4800	1.5244	1.5228	100	100	98
F ( H )	4861	1.5238	1.5224	100	100	99
e ( Hg )	5461	1.5192	1.5187	100	100	100
D ( Na: D1, D2 mean )	5893	1.5167	1.5167	100	100	100
HeNe laser	6328	1.5148	1.5151	100	100	100
C' ( Cd )	6439	1.5144	1.5147	100	100	100
C ( H )	6563	1.5139	1.5143	100	100	100
Ruby laser	6943	1.5127	1.5132	100	100	100
GaAs laser	8400	1.5094	1.5100	100	100	99
Nd: YAG laser	10648	1.507	1.507	100	100	98
Diode	13000	1.506	1.504	100	100	96
Diode	15500	1.505	1.501	100	99	90
$n_F - n_C$		=	0.0099			
Abbe $v_D : ( n_D - 1 ) / ( n_F - n_C )$		=	52.0			
Temp. Coef.: $dn_D / dt$ 15-35 °C		=	-0.000393			
<b>CARGILLE LABORATORIES</b> 55 Commerce Road, Cedar Grove, NJ 07009-1289 U.S.A. Phone: 973-239-6633 / Fax: 973-239-6096 / Email: Cargillelabs@aol.com						



**SECTION B-B**  
**SCALE 2 : 1**

**DETAIL D**  
**SCALE 1.5 : 1**

UNLESS OTHERWISE SPECIFIED:  
DIMENSIONS ARE IN MM  
TOLERANCES:  
FRACTIONAL ±  
ANGULAR MATCH ± BEND ±  
TWO PLACE DECIMAL ±  
THREE PLACE DECIMAL ±

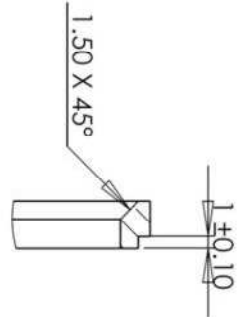
INTERPRET GEOMETRIC TOLERANCING PER:  
MATERIAL: Al 6061 T6  
FINISH: Black Anodize  
DO NOT SCALE DRAWING

DATE	NAME	TITLE:
		<b>Cell Barrel</b>

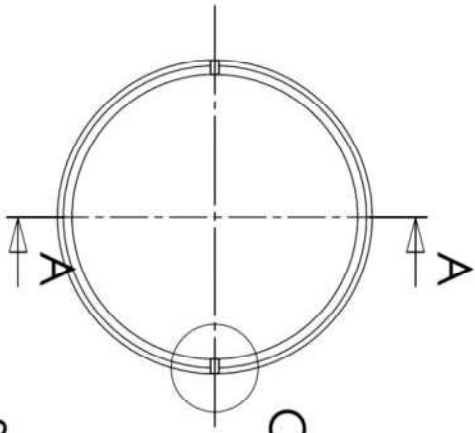
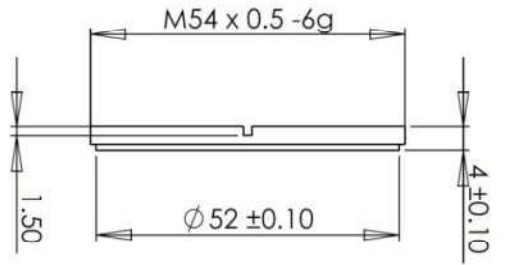
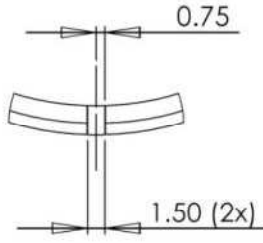
**PROPRIETARY AND CONFIDENTIAL:**  
THE INFORMATION CONTAINED IN THIS DRAWING IS THE SOLE PROPERTY OF...  
SOLIDWORKS CORPORATION  
171 Cambridge Street  
Boston, MA 02142  
TEL: 617 552 3500  
WWW.SOLIDWORKS.COM

APPLICATION	USED ON	FINISH	SCALE	DATE	REV
4		Black Anodize	1:1		

**SolidWorks Student License**  
**Academic Use Only**



**DETAIL B**  
SCALE 2 : 1



**SECTION A-A**

**DETAIL C**  
SCALE 2 : 1

**PROPRIETARY AND CONFIDENTIAL**  
THE INFORMATION CONTAINED IN THIS DRAWING IS THE SOLE PROPERTY OF <INSERT COMPANY NAME HERE>. ANY REPRODUCTION IN PART OR AS A WHOLE WITHOUT THE WRITTEN PERMISSION OF

**SolidWorks Student License**  
Academic Use Only

UNLESS OTHERWISE SPECIFIED:		DRAWN	NAME	DATE
DIMENSIONS ARE IN INCHES				
FRACTIONAL		CHECKED		
ANGULAR: MACH ±		ENG APPR.		
TWO PLACE DECIMAL ±		MFG APPR.		
THREE PLACE DECIMAL ±		Q.A.		
INTERPRET GEOMETRIC TOLERANCING PER		COMMENTS:		
MATERIAL: <b>BRASS</b>				
FINISH				
DO NOT SCALE DRAWING				
APPLICATION	USED ON			
4				
NEXT ASSY				
TITLE:		Retaining Ring		
SIZE: <b>A</b>		DWG. NO.		REV
SCALE: 1:1		WEIGHT:		SHEET 1 OF 1

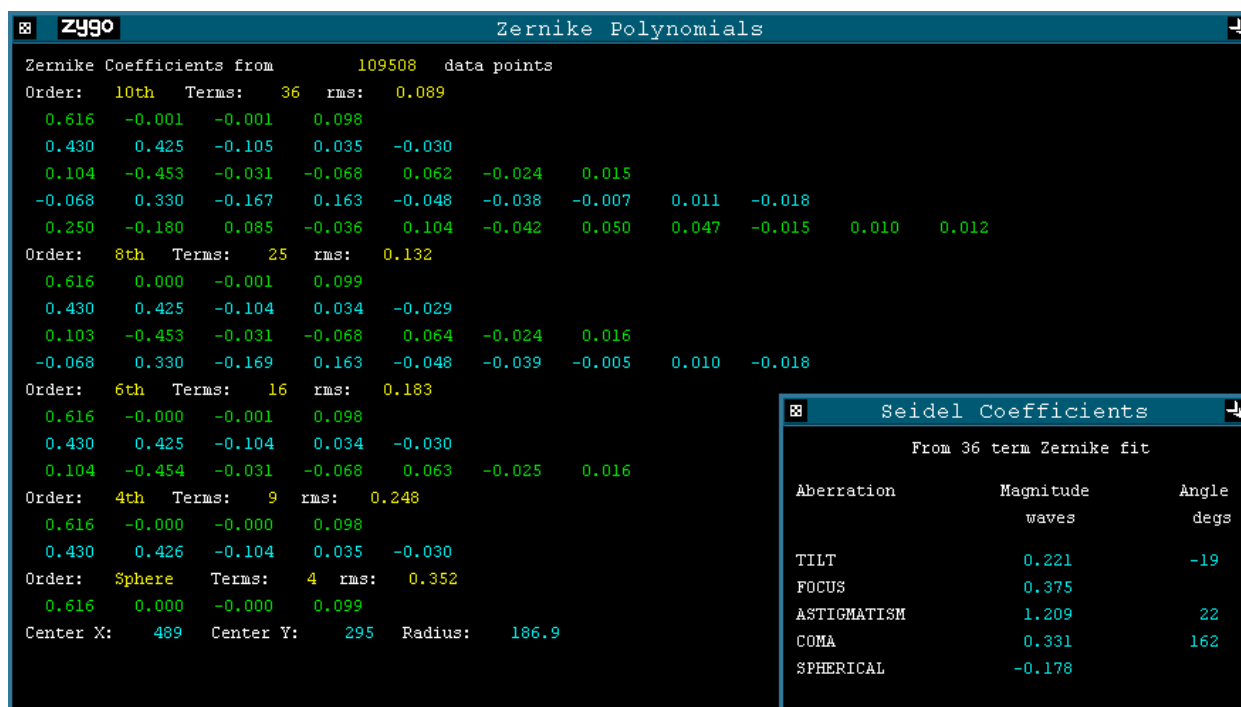


Figure 11: Zernike terms and Seidels for ambient measurement #1

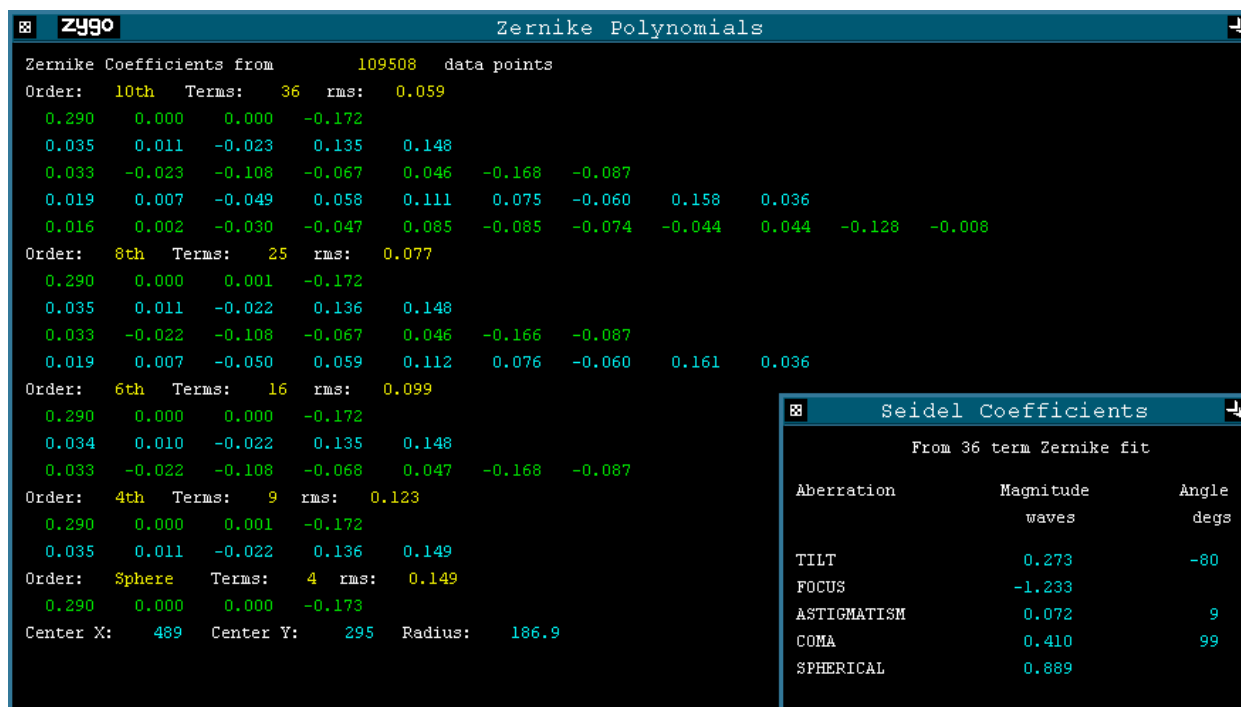


Figure 12: Zernike terms and Seidels for 40°C measurement #1

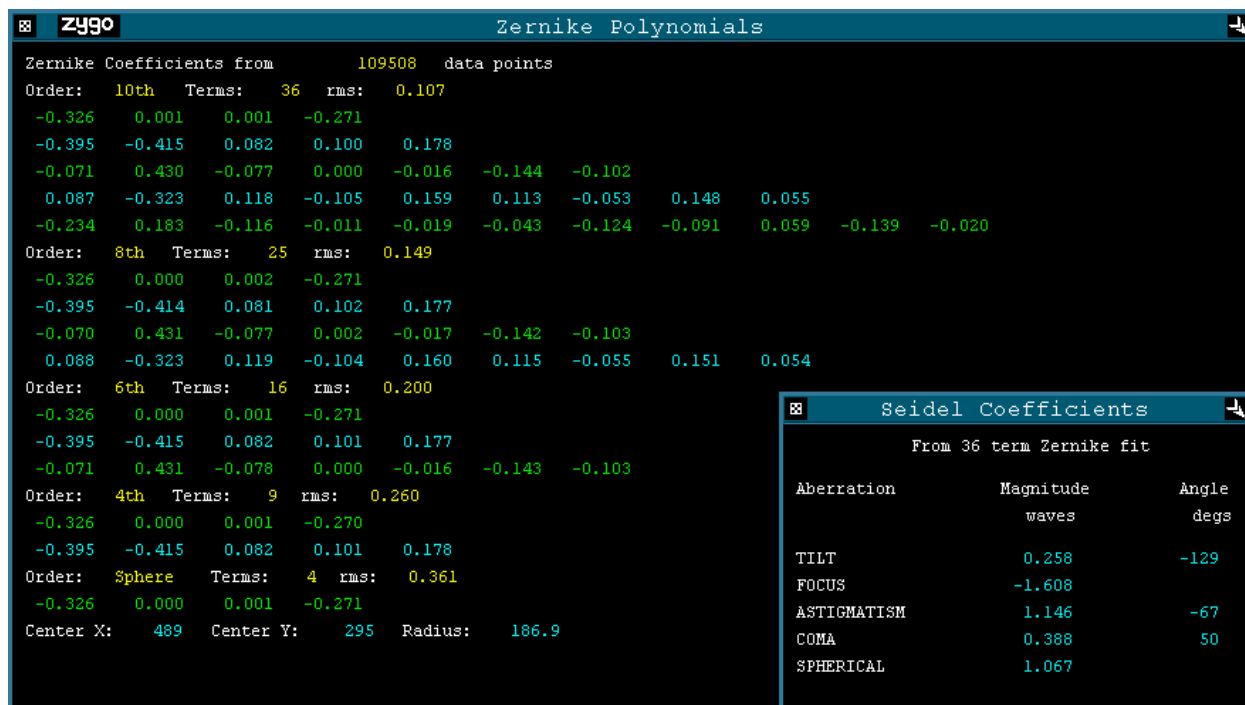


Figure 13: Zernike terms and Seidels for subtracted result #1

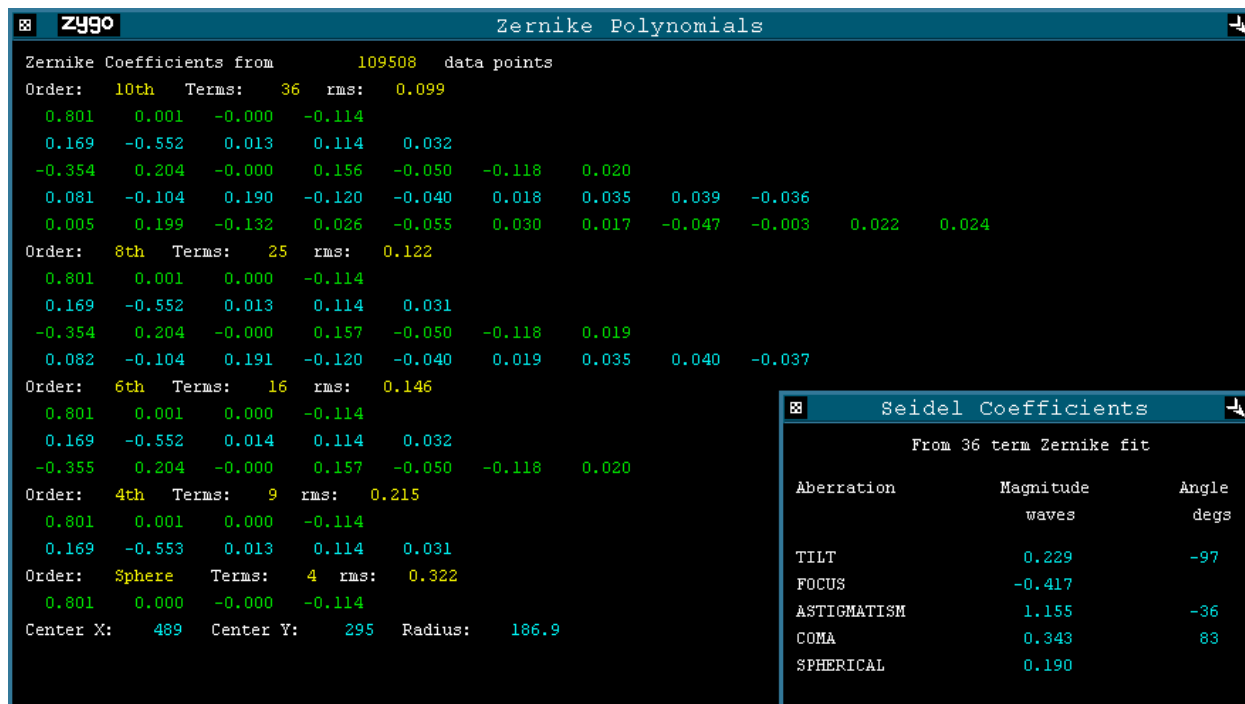


Figure 14: Zernike terms and Seidels for ambient measurement #2

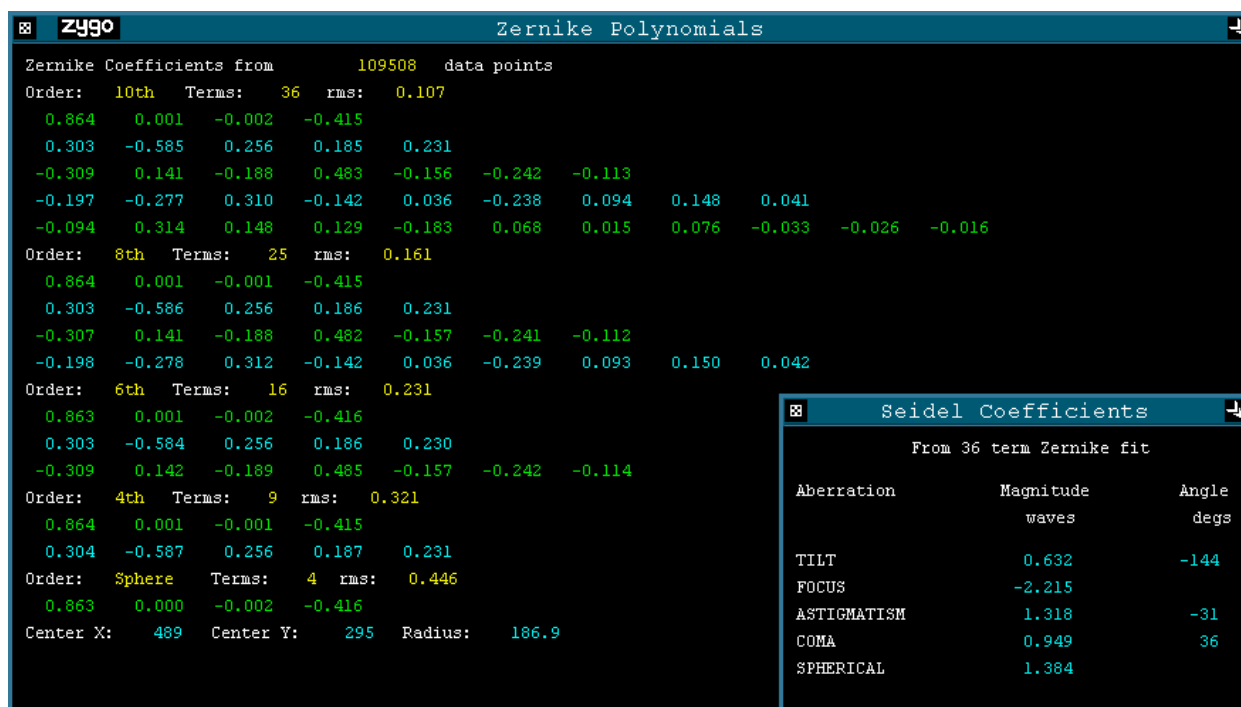


Figure 15: Zernike terms and Seidels for 40°C measurement #2

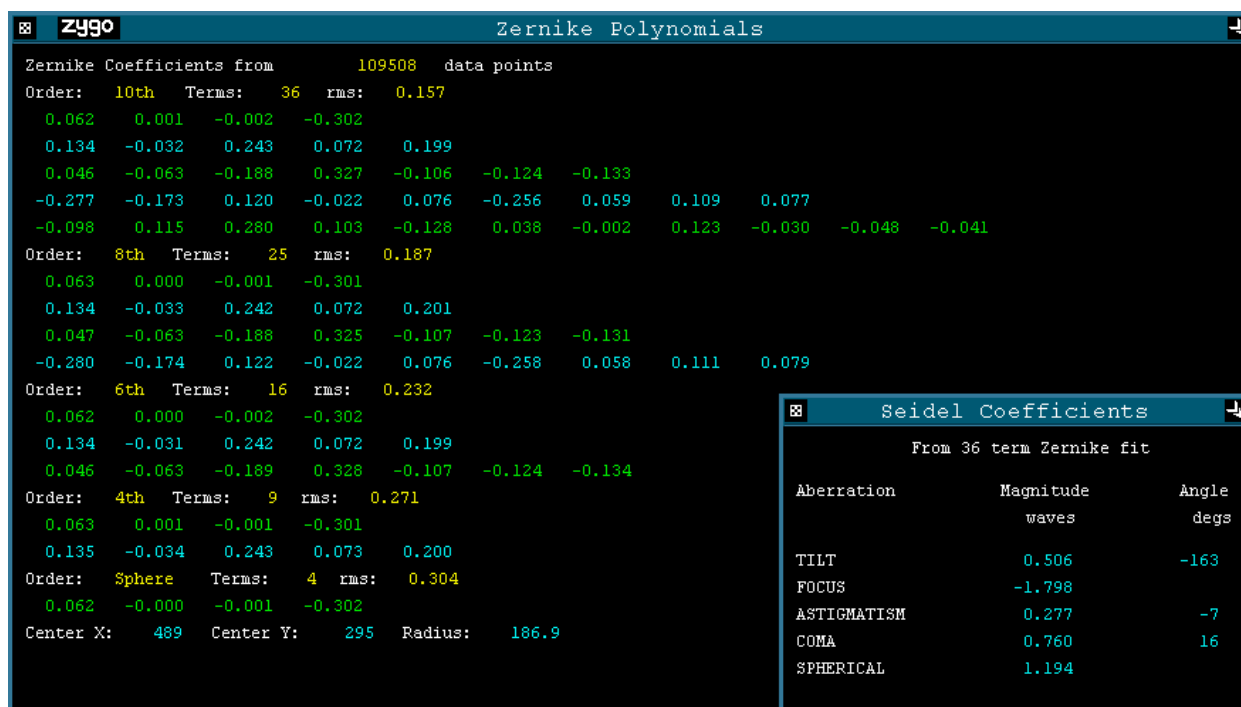
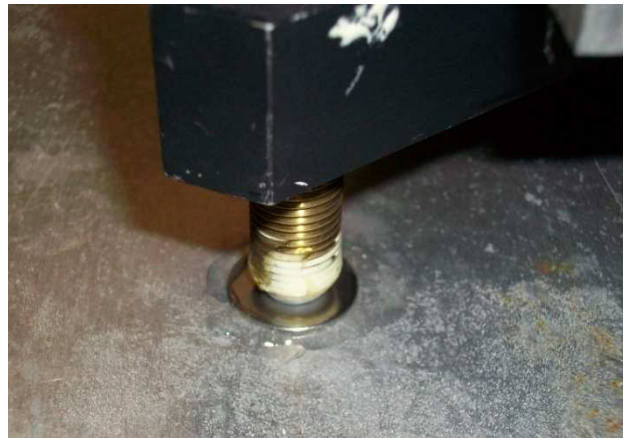


Figure 16: Zernike terms and Seidels for subtracted result #2

## Thermal chamber construction and features



**Figure 17: Mounting plate with isolation posts**



**Figure 18: Adjustment screw of mounting plate**



**Figure 20: Thermal chamber platform and mounting plate showing stainless steel posts and plastic isolation balls**

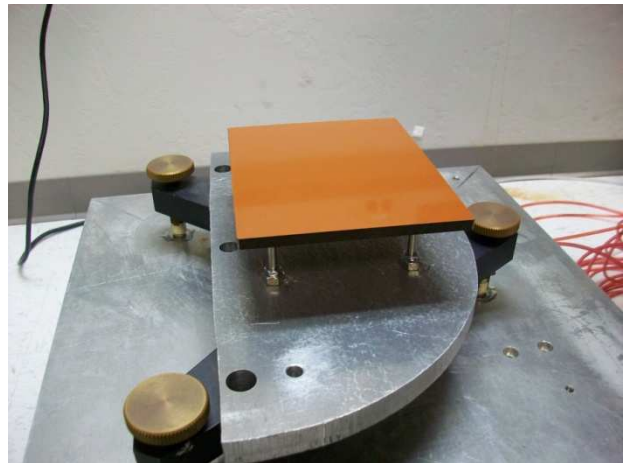


**Figure 19: Mounted thermal chamber platform**

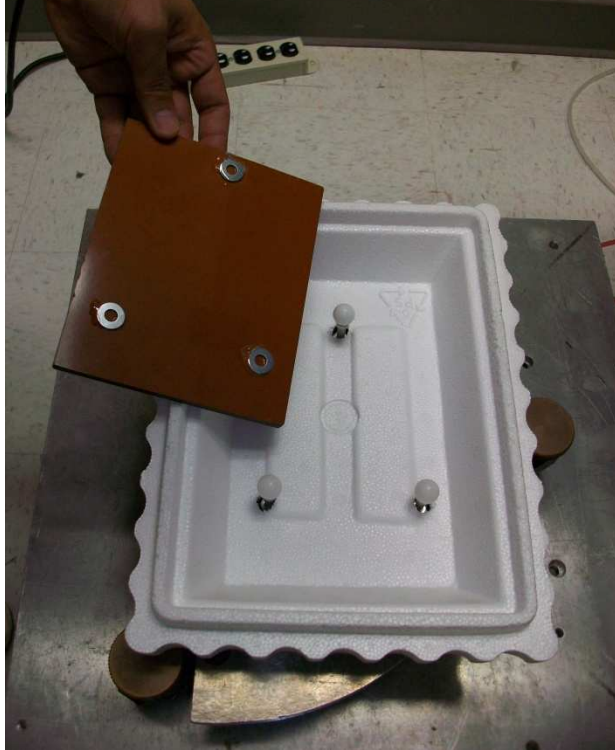


**Figure 21: Base of thermal chamber showing isolation posts and platform**

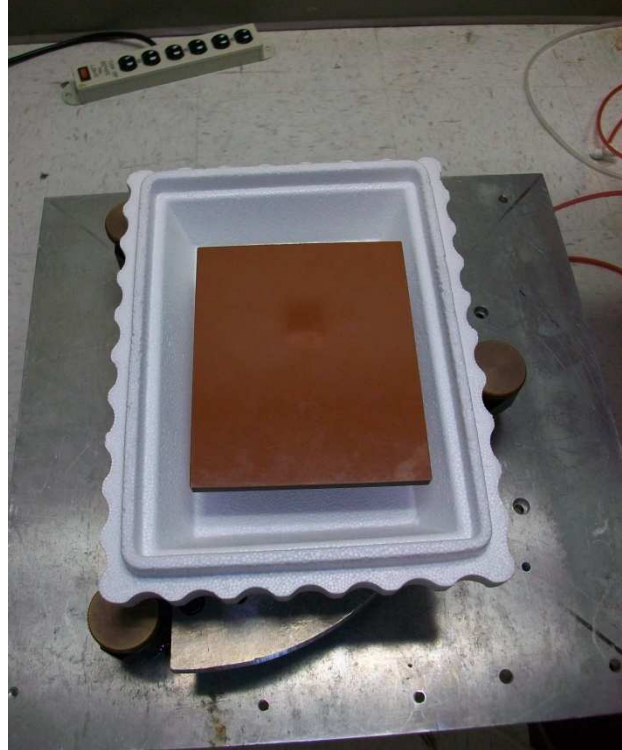


**Figure 22: Platform secured in thermal chamber base**

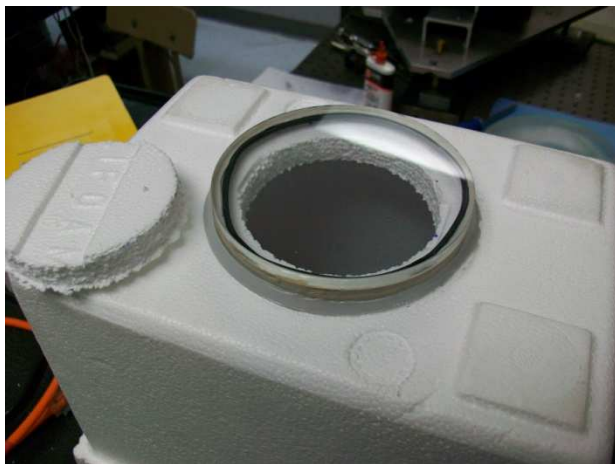


**Figure 24: Double-paned thermal chamber window**

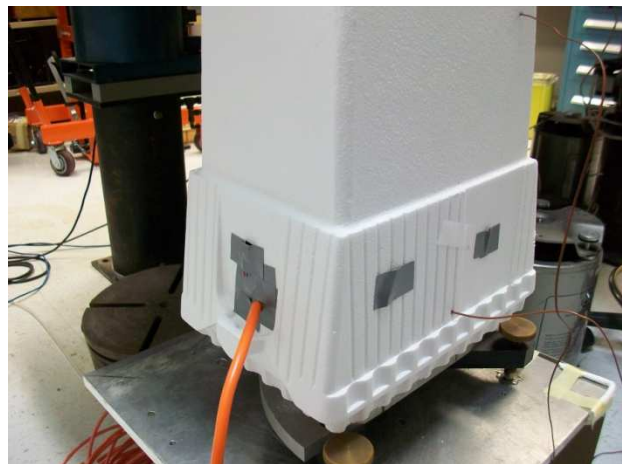


**Figure 23: Thermal chamber with heating element power core and thermocouple wires showing**



**Figure 26: Inside of thermal chamber showing heating element**

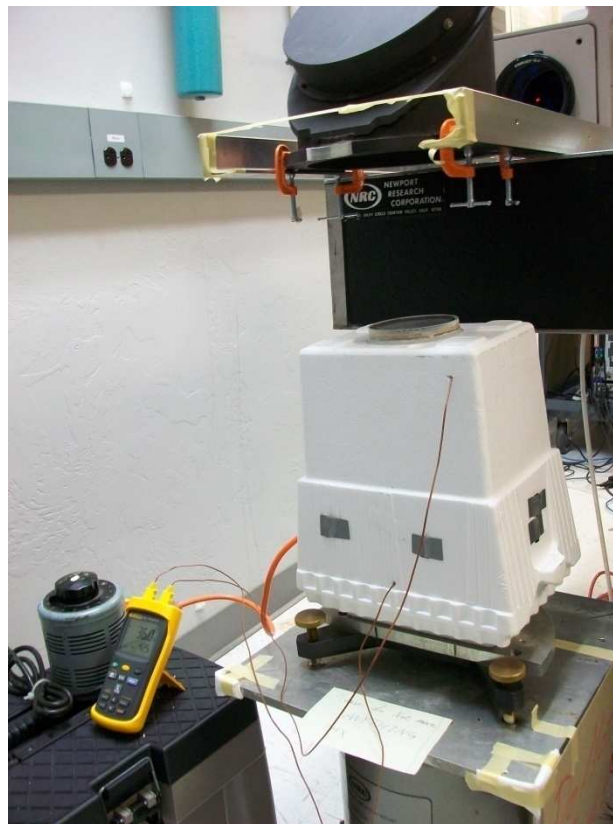


**Figure 25: Thermal chamber , temperature controller and monitor, fold mirror and interferometer**

## 10. References

Paul R. Yoder Jr., “*Opto-Mechanical System Design, Third Edition*”, CRC Press, Taylor & Francis Group, 2006

‘Apochromatic Color Correction Using Liquid Lenses’ – Robert D. Sigler, Applied Optics Vol. 29, No. 16 1990

Specialty Optical Liquids catalogue – Cargille Laboratories Inc., Cedar Grove NJ 07009